The exchange bias phenomenon in uncompensated interfaces: theory and Monte Carlo simulations

2011 J. Phys.: Condens. Matter 23 386004

(http://iopscience.iop.org/0953-8984/23/38/386004)

IOP PUBLISHING JOURNAL OF PHYSICS: CONDENSED MATTER

J. Phys.: Condens. Matter **23** (2011) 386004 (10pp) doi:10.1088/0953-8984/23/38/386004

The exchange bias phenomenon in uncompensated interfaces: theory and Monte Carlo simulations

O V Billoni, S A Cannas and F A Tamarit

Facultad de Matemática Astronomía y Física, Universidad Nacional de Córdoba and Instituto de Física Enrique Gaviola (IFEG-CONICET), Ciudad Universitaria, 5000 Córdoba, Argentina

E-mail: billoni@famaf.unc.edu.ar, cannas@famaf.unc.edu.ar and tamarit@famaf.unc.edu.ar

Received 20 April 2011, in final form 11 August 2011
Published 8 September 2011
Online at stacks.iop.org/JPhysCM/23/386004

Abstract

We performed Monte Carlo simulations of a bilayer system composed of two thin films, one ferromagnetic (FM) and the other antiferromagnetic (AFM). Two lattice structures for the films were considered: simple cubic and body centered cubic (bcc). We imposed an uncompensated interfacial spin structure in both lattice structures; in particular we emulated an FeF_2–FM system in the case of the bcc lattice. Our analysis focused on the incidence of the interfacial strength interactions between the films, J_{eb}, and the effect of thermal fluctuations on the bias field, H_{EB}. We first performed Monte Carlo simulations on a microscopic model based on classical Heisenberg spin variables. To analyze the simulation results we also introduced a simplified model that assumes coherent rotation of spins located on the same layer parallel to the interface. We found that, depending on the AFM film anisotropy to exchange ratio, the bias field is controlled either by the intrinsic pinning of a domain wall parallel to the interface or by the stability of the first AFM layer (quasi-domain wall) near the interface.

(Some figures in this article are in colour only in the electronic version)

1. Introduction

Exchange bias (EB) is a ubiquitous magnetic phenomenon that usually appears when two different magnetic media are in contact. Although EB can be observed in a large variety of non-homogeneous magnetic materials [1, 2], in this work we will focus on the case of a bilayer system composed of two films, one ferromagnetic (FM) and the other antiferromagnetic (AFM).

Assuming that the Curie temperature T_C of the FM material is larger than the Néel temperature T_N of the AFM one, and that the two films are magnetically coupled by exchange interactions, an unusual hysteresis phenomenon can be observed. If such a system is cooled down below T_N in the presence of an external applied magnetic field H_{CF}, the hysteresis loops of the FM material evidence three important anomalies when compared with the loop of the single FM film. First, a shift in the loop appears, characterized by a new center called the bias field H_{EB}. This shift is due to the unidirectional anisotropy induced at the interface. Second, the width of the loop usually increases. Finally, the loop also loses its symmetry. As temperature increases, the bias field H_{EB} goes to zero at a certain blocking temperature T_B, with $T_B < T_N$, restoring the normal hysteresis loop of the isolated ferromagnet.

Although this phenomenon was reported for the first time in 1956 [3] and despite the huge theoretical and experimental effort devoted to understanding its origins, there are still many controversial points concerning the underlying mechanisms responsible for such unusual hysteresis anomalies [1, 2, 4–6]. In particular, these controversies are in part related to the fact that EB has been observed in a great diversity of magnetic systems, including for instance spin glasses, and intrinsic inhomogeneous and nanoparticle systems, as well as the bilayered system analyzed in this paper. Beyond the theoretical interest, this phenomenon is also relevant because of its technological applications—for instance, in the design

of magnetic sensor and magnetic recording media devices [2], among many others.

As regards the case of a bilayered FM/AFM system, the spin structure at the interfacial planes is a main issue in developing the understanding of the EB phenomenon. In particular, AFM interfaces can be roughly classified as *compensated* or *uncompensated*, depending on whether the nearest AFM planes parallel to the interface have zero net magnetization or not, respectively. Most of the earlier models that explain EB assume an uncompensated interfacial spin structure [4], even when this requirement is not always fulfilled in experiments. Actually, EB can also be observed in compensated interfaces, but in this case the existence of uncompensated domains has proved to be fundamental for the appearance of the hysteresis shift [7]. Furthermore, fully uncompensated interfaces can manifest a weaker EB field when compared with partially uncompensated or even compensated interfaces. In fact, experiments carried out by Moran *et al* [8] and Nogués *et al* [9] on Fe films grown over FeF_2 single crystals cut along different orientations showed that H_{EB} is larger when the interface is compensated ((110) plane) in comparison with the uncompensated case ((010) plane). This effect is supposed to be associated with spin rearrangement at the interface [2, 9] since a similar behavior was found when the AFM is a single crystal or a thin film.

A key point for the understanding of the EB phenomenon on uncompensated interfaces is the effect of the variation of the exchange coupling between interface layers on the EB field. While it is difficult to control this quantity at the experimental level, this problem can be handled easily using Monte Carlo simulations based on microscopic models. In addition, this methodology allows a detailed description of the interfacial spin structure together with the incorporation of thermal fluctuations, which are relevant for the stability and therefore the appearance of the EB phenomenon. For instance, thermal effects are necessary to explain the widening of the hysteresis loop close to the blocking temperature [10–12]. In this sense, numerical studies at the micromagnetic [13–15] and Monte Carlo simulation levels [16–23] have proved to be very useful tools for modeling realistic systems. On the other hand, the continuous approximation assumed in micromagnetic based models breaks down for highly anisotropic materials like FeF_2–AFM compounds. Discretization could give rise to different energy barriers with the consequent thermal activated effects [24]. Hence, atomic scale based models could be crucial for getting an appropriate description of the magnetic properties.

In this paper we analyze the EB phenomenon in an FM–AFM bilayer system with an uncompensated interface. In section 2 we summarize the existing theoretical background, discussing the phenomenology of the EB system in the framework of two of the most relevant models. In section 3 we introduce a microscopic model for the bilayered system, describe the simulation protocol and show our numerical results. In order to interpret the results of the previous section we introduce in section 4 a generalization of the Meiklejohn–Bean model, which allowed us to analyze the role of the AFM layers in the EB phenomenon. In section 5 we summarize and discuss the results.

2. The theoretical background

In order to analyze the role of the strength of the interface exchange interaction J_{eb} in the behavior of bias field H_{eb}, let us discuss first the following question: what happens with the order of the antiferromagnet as we invert the orientation of the ferromagnet magnetization by applying an opposite magnetic field h? We assume that the system has already reached thermal equilibrium at a certain temperature T below T_B, in such a way that, if J_{eb} were zero, both films would have achieved an ordered state. Since $T_C > T_N$, we assume that $|J_F| > |J_A|$ where J_F and J_A are the exchange interactions of the ferromagnet and antiferromagnet, respectively. If J_{eb} is small enough ($J_{eb} \ll J_A$) the spins in the antiferromagnet will remain almost insensitive to the rotation of the global magnetization of the FM film. In this case the Meiklejohn–Bean model [25] predicts a linear dependence of the bias field H_{eb} on the value of J_{eb}:

$$H_{EB} \propto \frac{J_{eb}}{L_{FM}}, \tag{1}$$

where L_{FM} is the thickness of the FM film.

At the other extreme, when J_{eb} is large enough, the rotation of the magnetization would induce the creation of a domain wall (parallel to the interface) in the AFM films, at least for small enough values of K_A. Once a perfect domain wall has been formed, any increase of J_{eb} will not alter the value of H_{eb}. This phenomenology is captured by the model of Mauri *et al* [26] (from now on the MSBK model) when the anisotropy of the FM film is negligible. This model predicts an initial increase of H_{eb} with J_{eb} for small values of J_{eb}, followed by a saturation for large enough values of J_{eb} at

$$H_{EB} = 2\frac{\sqrt{\omega J_A K_A}}{L_{FM}}, \tag{2}$$

where K_A is the anisotropy constant of the antiferromagnet and ω is a constant depending on the lattice structure. The previous results suggest a monotonic behavior of the bias field when the anisotropy of the FM film is negligible, with a linear dependence of H_{eb} on J_{eb} for small values of J_{eb} and a saturation for large values of it. As we will show in the next section, such a scenario can change substantially depending on the effective anisotropy of the AFM film.

3. The microscopic model and numerical simulations

3.1. The microscopic model

We considered an FM film mounted over an AFM film as depicted in figure 1(a). The films are magnetically coupled to each other by exchange interactions and the structure of both films is either bcc or sc, assuming a perfect match across the FM/AFM interface. The system is ruled by the following

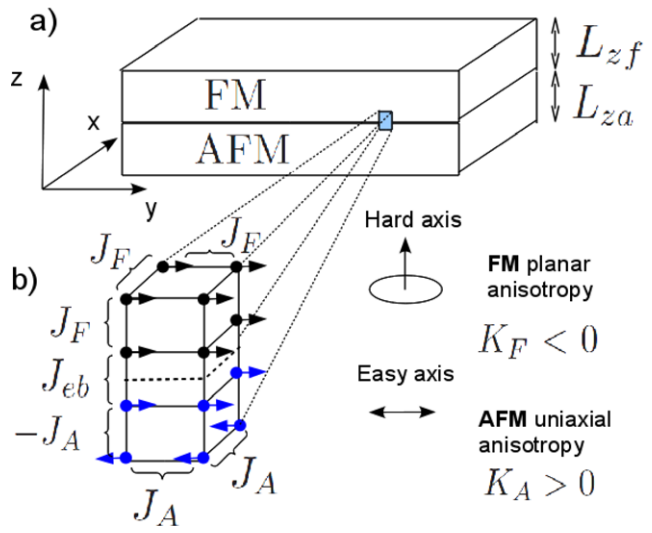

Figure 1. (a) Scheme of the bilayer system including the reference frame used throughout this paper. (b) Schematic picture of the system modeled by the Hamiltonian (3) in the sc lattice case. Here we show the ground state configuration with the corresponding interactions.

Hamiltonian:

$$H = -J_{\rm F} \sum_{\langle \vec{r},\vec{r}'\rangle \in {\rm FM}} \vec{S}_{\vec{r}} \cdot \vec{S}_{\vec{r}'} - K_{\rm F} \sum_{\vec{r}\in {\rm FM}} (S^z_{\vec{r}})^2 - \sum_{\langle \vec{r},\vec{r}'\rangle \in {\rm AFM}} J_{\rm AF}(\vec{r}-\vec{r}')\vec{S}_{\vec{r}} \cdot \vec{S}_{\vec{r}'} - K_{\rm A} \sum_{\vec{r}\in {\rm AFM}} (S^y_{\vec{r}})^2 - J_{\rm eb} \sum_{\langle \vec{r},\vec{r}'\rangle \in {\rm FM/AFM}} \vec{S}_{\vec{r}} \cdot \vec{S}_{\vec{r}'} - h \sum_{\vec{r}} S^y_{\vec{r}}, \quad (3)$$

where $\vec{S}_{\vec{r}}$ is a classical Heisenberg spin ($|\vec{S}_{\vec{r}}| = 1$) located at the node $\vec{r}$ of the lattice. $\langle \vec{r}, \vec{r}\,' \rangle$ denotes a sum over nearest-neighbor pairs of spins, $J_{\rm F} > 0$ is the exchange constant of the ferromagnet and $J_{\rm AF}(\vec{r} - \vec{r}')$ is the strength of the AFM exchange interactions which explicitly depends on the vector $r - r'$. This dependence of $J_{\rm AF}$ on $\vec{r} - \vec{r}'$ is introduced in order to set an uncompensated interface at the antiferromagnet. For the bcc lattice we set $J_{\rm AF} = -J_{\rm A}$ with $J_{\rm A} > 0$ for all pairs $(\vec{r}, \vec{r}')$, while for the sc lattice we set $J_{\rm AF} = J_{\rm A}$ if the $(\vec{r}, \vec{r}')$ belong to the same plane parallel to the interface and $J_{\rm AF} = -J_{\rm A}$ otherwise (see figure 1(b)). $J_{\rm eb} > 0$ represents the exchange coupling between the FM and the AFM interface layers of the films, $K_{\rm F}$ is the anisotropy constant of the ferromagnet, $K_{\rm A}$ is the AFM anisotropy and h is an external homogeneous magnetic field oriented along the y direction. We assumed that:

(i) $K_{\rm F} < 0$ in order to ensure that the FM anisotropy term tends to align the spins on the plane of the film, mimicking the dipolar shape anisotropy, as usual [23, 24];

(ii) $K_{\rm A} > 0$ in order to introduce a uniaxial anisotropy along the y direction in the AFM material [18].

We carried out Monte Carlo simulations using the Metropolis algorithm and Hamiltonian (3). In our simulations

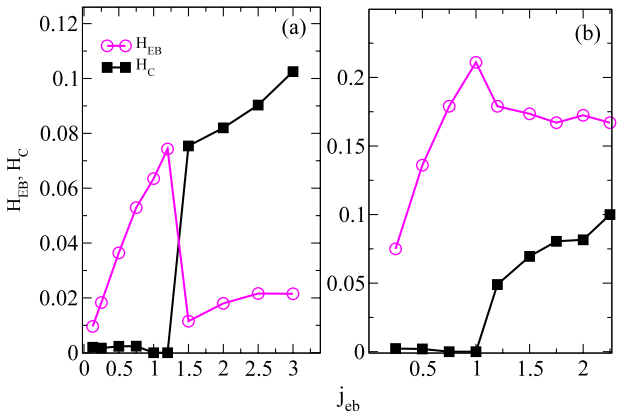

Figure 2. Bias field $H_{\rm EB}$ (circles) and coercivity $H_{\rm C}$ (squares) versus $j_{\rm eb}$ at $T/J_{\rm A} = 0.5$ and $K_{\rm A}/J_{\rm A} = 1.77$ for (a) an sc lattice and (b) a bcc lattice.

L_x and L_y are the lateral dimensions of the films, in units of the lattice parameter, and $L_{\rm za}$ and $L_{\rm zf}$ are the thicknesses of the FM and AFM films, respectively, measured in the same units. The total number of spins is then $N = \eta\, L_x\, L_y\, (L_{\rm za}+L_{\rm zf})$ where $\eta = 1$ (2) for the sc (bcc) lattice. Periodic boundary conditions were imposed in the plane of the film while we used open boundary conditions in the perpendicular direction to the film. For each point in the magnetization curve presented in this work, we took 10^4 Monte Carlo steps per site (MCS) to thermalize the system and then the same number of MCS to calculate the temporal averages of the magnetization. We follow the ideas used in [27, 28], where at each spin actualization the direction of the spin is adjusted in a cone in such a way as to maintain an acceptance rate close to 0.46. This is an approximation to a Landau–Lifshitz–Gilbert Langevin dynamics in the high damping limit [29]. We set the following dimensions for the system: $L_x = L_y = 40$ and $L_{\rm za} = L_{\rm zf} = 12$, and fix the following parameters: $J_{\rm F} = 9.56J$, $J_{\rm A} = -J$ and $K_{\rm F} = -0.5J$, where J is an arbitrary parameter that sets the energy units. $J_{\rm eb}$ varies in the interval $[0, J_{\rm F}]$ while $K_{\rm A}$ can take arbitrary values. With these parameters we can emulate a FeF_2–FM system in the bcc lattice by choosing $K_{\rm A} = 1.77J$ [18]. Since we are interested in the high AFM anisotropy to exchange ratio regimen, which implies small domain wall width, the thickness of the antiferromagnet that we chose is enough for supporting an AFM domain wall. On the other hand, it is known that in this model [18, 30] for such sizes both the AFM and the FM films reach an ordered state.

3.2. Results

In figure 2 we present the bias field $H_{\rm EB}$ (open circles) and coercivity $H_{\rm C}$ (squares) obtained from Monte Carlo simulations as functions of the interfacial interaction strength $J_{\rm eb}$ for the two lattice structures considered and for fixed values of the temperature and AFM anisotropy. When the interfacial exchange coupling $j_{\rm eb} \equiv J_{\rm eb}/J_{\rm A}$ is weak, $H_{\rm EB}$ shows, for both lattice structures, a linear dependence, indicating that the AFM spins located near the interface are fixed, and the FM film reverses its magnetization by

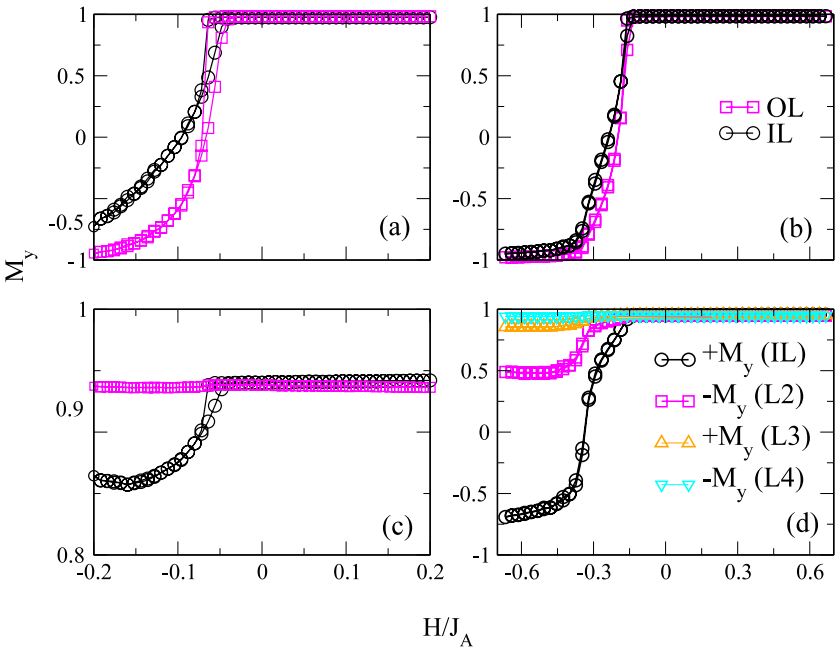

Figure 3. Hysteresis loops of several atomic layers of the bilayer corresponding to the FM planes (top) and AFM planes (bottom) for $j_{eb} = j_{eb}^{max}$ and $T/J_A = 0.5$. The panels on the left ((a) and (c)) correspond to the sc lattice and the panels on the right ((b) and (d)) correspond to the bcc lattice. See the text for details.

coherent rotation [16]. As j_{eb} increases, the bias field reaches a maximum value at j_{eb}^{max} and then abruptly drops to an almost constant value. Notice that the drop is larger for the sc lattice than for the bcc one. As will be shown later, such an effect is due to a reduction of the effective anisotropy of the AFM layer in the bcc case.

In figure 3 we show the hysteresis loops of several planes of the FM and AFM films. These loops were obtained at $j_{eb} = j_{eb}^{max}$, just before the drastic drops observed for H_{eb} in figure 2, where the exchange bias effect is more pronounced and the cycles are still almost reversible.

In figures 3(a) and (b) we present the magnetization in the interfacial (IL) and outer (OL) atomic layers of the FM film. These results show that, in the two lattices, the spins rotate almost coherently. In figures 3(c) and (d) we show the loops of the four AFM layers nearest to the interface (Ln stands for the nth atomic layer). Comparing the behaviors of the two structures we see that the sc lattice is more flexible than the bcc one inside the ferromagnet, but more rigid inside the antiferromagnet, because the effective anisotropy in the sc lattice is larger. In particular, in the AFM film of the sc case (figure 3(c)) only the first layer feels the effect of the FM film. In the bcc case (figure 3(d)) we clearly see the formation of a quasi-domain wall.

In figure 4 we plot the same quantities as in figure 3 for a value of j_{eb} above the peak, where the bias field has already diminished abruptly. Unlike in the previous case (figure 3), here the AFM layers show hysteresis behavior for both the sc and the bcc lattices (figures 4(c) and (d) respectively). This indicates that the drop in the bias field is associated with the onset of irreversible changes in the magnetic dynamics. As occurred below the peak (figure 3), the changes in the antiferromagnet are constrained to the first planes near the interface. It is worth stressing that now the hysteresis phenomenon also appears in the AFM layers, as evidenced in the behavior of the coercivity in figure 2.

Next we analyzed the temperature dependence of the overall magnetic behavior. In figure 5 we present the bias field H_{EB} and the coercivity H_C as a function of temperature for two values of the interfacial interaction strength: $j_{eb} = 0.5$ (figures 5(a) and (b)) and 1.0 (figures 5(c) and (d)). The panels on the left correspond to the sc lattice and panels on the right to the bcc lattice. The dotted lines represent the staggered magnetization of the antiferromagnet at zero external magnetic field, normalized with respect to the value of the bias field at the lowest temperature. In figures 5(b)–(d) we observe that the system presents a blocking temperature T_B separating two phases with different magnetic behaviors. At low temperature the system is characterized by the presence of exchange bias and almost zero coercivity. On the other hand, for $T_B < T < T_N$ the bias disappears and the H_C increases and further decays following the behavior of the normalized staggered magnetization. A completely different behavior is observed in figure 5(a), where the ordered phase coincides with the bias regime and therefore $T_B = T_N$. In this case we do not observe any trace of coercivity in the simulations. Note that for both structures, sc and bcc, the blocking temperature decreases with the interfacial interaction strength, indicating that the energy barrier for depinning the partial domain wall decreases as the wall approaches a 180° domain wall.

Finally we explored the effect of the lattice structure on the bias field. The main difference between the two lattice structures lies in the number of nearest neighbors belonging to adjacent layers of any site in the AFM film, which is four times larger in the bcc than in the sc structure. Hence, one would expect the effective anisotropy to be reduced by a factor

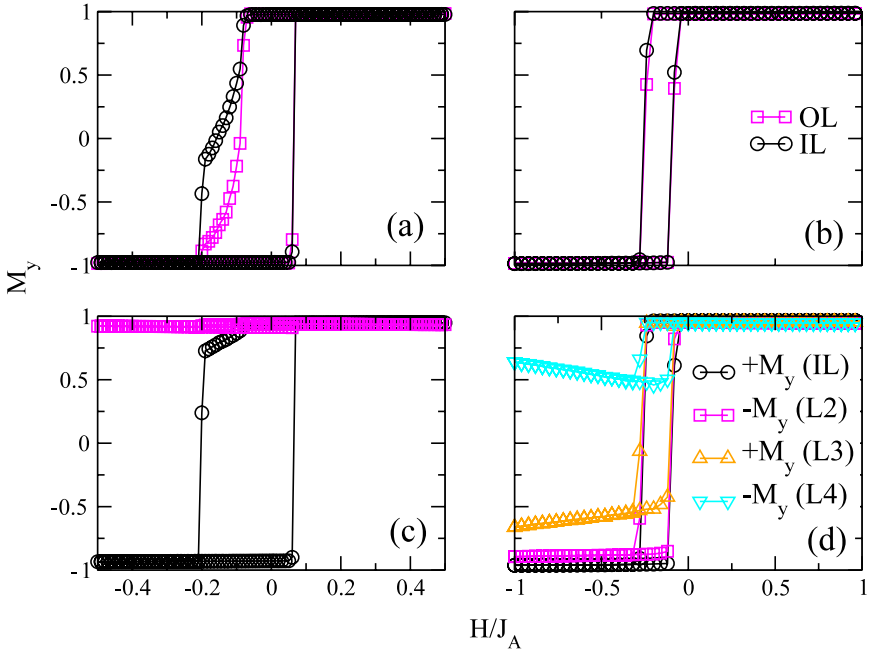

Figure 4. Hysteresis loops of several atomic layers of the bilayer corresponding to the FM planes (top) and AFM planes (bottom) for $j_{eb} = 2$ and $T/J_A = 0.5$. The panels on the left ((a) and (c)) correspond to the sc lattice and the panels on the right ((b) and (d)) correspond to the bcc lattice.

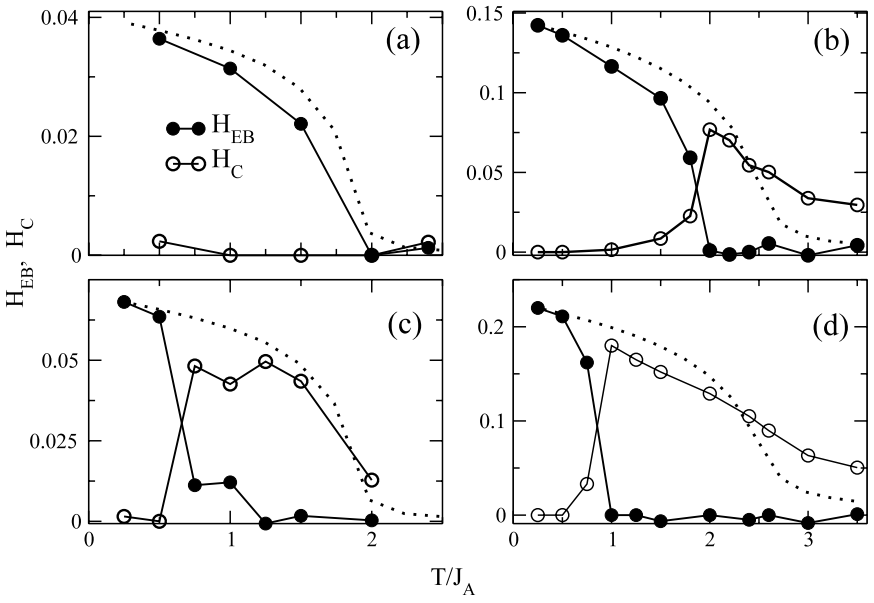

Figure 5. H_{EB} and H_C versus T/J_A for $K_A/J_A = 1.77$ and two interfacial exchange interactions: top, $j_{eb} = 0.5$ ((a) and (b)) and bottom, $j_{eb} = 1$ ((c) and (d)). Left: sc lattices ((a) and (c)); right: bcc lattices ((b) and (d)). The dotted lines represent the staggered magnetization of the antiferromagnet at zero external magnetic field, normalized with respect to the value of the bias field at the lowest temperature.

of 4 in the bcc lattice with respect to the sc one, while the bias field is expected to be four times larger in the bcc than in the sc case. To check this hypothesis we calculated the bias field as a function of j_{eb} for both lattices for the same value of $K' = K_A/\alpha J_A$, with $\alpha = 4$ for the bcc lattice and $\alpha = 1$ for the sc lattice. In order to compare the results, one has to take into account that the Curie temperatures are different for the two lattice structures. Hence, both calculations were carried out keeping T/T_c constant. In figure 6 we plot H_{eb}/α as a function of j_{eb} for high and low values of K'. For large enough values of the anisotropy the previous conjecture is verified, namely, the only effect of changing the lattice structure is a rescaling of the bias field and the effective anisotropy. For small values of the anisotropy, such scaling is observed as long as no hysteresis effects appear, namely, for small enough values of the coupling j_{eb}. For large values of j_{eb} the bias field exhibits only a small drop and it saturates at a constant value in the bcc lattice, but it drops to zero in the sc case. We observed that so

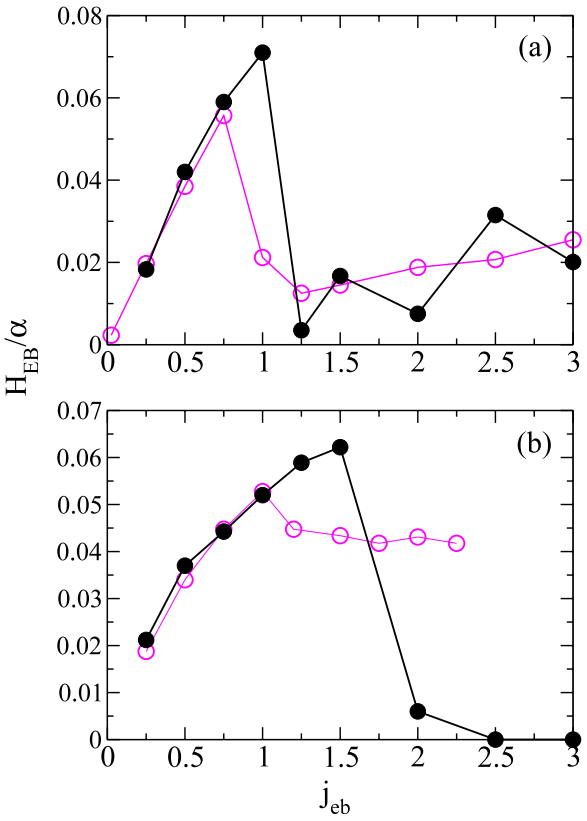

Figure 6. H_{EB}/α versus j_{eb} for $T/T_c = 0.14$ and different values of $K' = K_A/\alpha J_A$. Open symbols: bcc lattice. Filled symbols: sc lattice. (a) $K' = 1.77$. (b) $K' = 0.4425$.

large a drop is due to the depinning of the quasi-domain wall, i.e. to a complete reversion of the staggered magnetization at the AFM film. This effect is not observed in the bcc lattice (at least for the range of parameter values analyzed here). It is due to a reduction in the in plane magnetization component at the AFM layers, associated with a canting of the spins which enhance the pinning of the wall.

4. The layered model

As we have seen in section 3, the behavior of the bias field is strongly determined by the magnetization dynamics of the atomic layers close to the interface. Moreover, we observed that, for reasonably large values of the anisotropy, the spins in each layer rotate almost coherently under the application of an external field parallel to the interface. On the basis of these observations, we introduced a generalization of the Meiklejohn–Bean [25] model that explicitly includes the contribution of the AFM layers close to the interface. We consider that only the n layers of the AFM film closest to the interface are free to move, while the rest of the AFM layers retain the equilibrium AFM configuration of the bulk at temperature T. Let $\vec{S}$ and $\vec{\sigma}_j$ be the average magnetization per layer per unit area at the ferromagnet and the antiferromagnet jth layers respectively. $\vec{S}$ and $\vec{\sigma}_j$ $(j = 1, \ldots, n)$ are assumed to be unit vectors parallel to the interface. The magnetization per unit area of the whole FM film is then given by $L_{FM}\vec{S}$

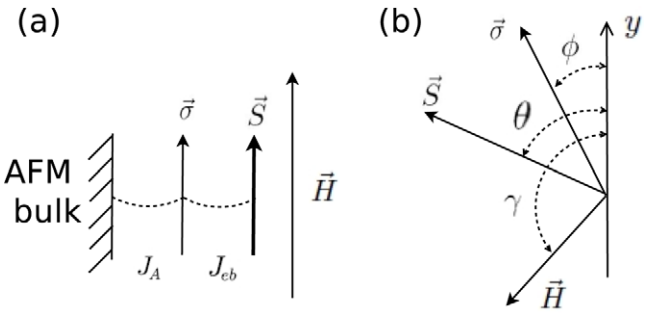

Figure 7. (a) Scheme of the model for $n = 1$ (equation (5)). (b) Angles representing the state of the system.

(with L_{FM} the FM film thickness), since we are assuming a coherent rotation of the whole FM film. The nth layer is the closest one to the interface. We assume that the applied field $\vec{H}$ is parallel to the interface and only interacts with the FM film. This approximation is valid as long as the applied field is small enough compared with the molecular field of the aniferromagnet. Finally, we consider the anisotropy of the antiferromagnet to be much larger than the FM one, so the latter can be neglected. The Hamiltonian of the model is then given by

$$\mathcal{H}_n = -K_A \sum_{i=1}^{n} (\sigma_i^y)^2 + (-1)^n \alpha J_A \sigma_0(T) \sigma_1^y + \alpha J_A \sum_{i=1}^{n-1} \vec{\sigma}_i \cdot \vec{\sigma}_{i+1} - J_{eb} \vec{\sigma}_n \cdot \vec{S} - \vec{H}' \cdot \vec{S}, \quad (4)$$

where $\vec{H}' = L_{FM}\vec{H}$, $\alpha = 4$ $(\alpha = 1)$ for the bcc (sc) lattice and $\sigma_0(T)$ is the average equilibrium magnetization per unit area of one layer in the AFM bulk, assumed to be parallel to the easy axis. The $(-1)^n$ factor in the second term of equation (4) ensures the correct equilibrium configuration at zero temperature and magnetic field with the $n-1$ AFM spins aligned with the FM spin. The model is then equivalent to a $n+1$-spin chain, where the first spin in the chain is subjected to a local effective field produced by ordering in the AFM bulk, while the spin located at the end of the chain ($\vec{S}$) represents the FM film which interacts with an external magnetic field and is ferromagnetically coupled to the nth AFM spin.

At $T = 0$ the sublattice magnetization in the bulk is saturated, so we have $\sigma_0(T) = 1$. In a first approximation we can consider the simplest case of only one AFM layer free to move $n = 1$ (see figure 7(a)), which is enough to illustrate the general mechanism. The energy is then given by

$$E = -K_A(\sigma^y)^2 - \alpha J_A \sigma^y - \alpha J_{eb} \vec{\sigma} \cdot \vec{S} - \vec{H}' \cdot \vec{S}, \quad (5)$$

where $\vec{\sigma} \equiv \vec{\sigma}_1$. The FM and AFM spins can be expressed in terms of the angles ϕ and θ with respect to the easy axis direction y of the antiferromagnet, in our case the field cooling direction (figure 7(b)). Then

$$E = -K_A \cos^2\phi - \alpha J_A \cos\phi - \alpha J_{eb} \cos(\theta - \phi) - H' \cos(\theta - \gamma), \quad (6)$$

where the angle γ gives the applied field direction (figure 7(b). From now on, we will consider the applied field parallel to the easy axis direction ($\gamma = \pi$). In order to obtain the hysteresis loops and the bias field, the model is analyzed using standard procedures (see e.g. [31]). First, we set the partial derivatives $\partial_\theta E$ and $\partial_\phi E$ equal to zero in order to obtain the critical points:

$$\begin{aligned} 0 &= \alpha J_{\rm eb}\sin(\theta-\phi) - H^{'}\sin(\theta) \\ 0 &= -\alpha J_{\rm eb}\sin(\theta-\phi) + \alpha J_{\rm A}\sin\phi + K_{\rm A}\sin(2\phi) \end{aligned} \tag{7}$$

and then we look at the stability criteria, $\partial_{\theta\theta}e\,\partial_{\phi\phi}e - \partial_{\theta\phi}e^2 > 0$ and $\partial_{\theta\theta}e > 0$, to decide whether there is a minimum or not. It turns out that

$$\begin{aligned} &0 < \alpha J_{\rm eb}\cos(\theta-\phi) - H^{'}\cos\,\theta \\ &0 < \alpha J_{\rm eb}\cos(\theta-\phi)[\alpha J_{\rm A}\cos\phi \\ &\quad + 2K_{\rm A}\cos 2\phi] - H^{'}\cos\theta\times\ [\alpha J_{\rm eb}\cos(\theta-\phi) \\ &\quad + \alpha J_{\rm A}\cos\phi + 2K_{\rm A}\cos 2\phi]. \end{aligned} \tag{8}$$

For $J_{\rm A} = 0$ we recover to the Meiklejohn–Bean model (see [6] and references therein) and the bias field is given by

$$H^{'}_{\rm eb} = \alpha J_{\rm eb}\sqrt{1-\left(\frac{J_{\rm eb}}{2K_{\rm A}}\right)^2}, \tag{9}$$

provided that $J_{\rm eb} < K_{\rm A}$. In this range of $J_{\rm eb}$ the coercivity field is zero. For $J_{\rm eb}/K_{\rm A} > 1$ the bias field drops to zero, while the coercivity jumps to a finite value (see figure 8), due to the complete reversal of all spins in the AFM film. In the limit $K_{\rm A} = \infty$, equation (9) predicts a linear increase of $H^{'}_{\rm eb}$ with $J_{\rm eb}$ (see figure 8). This case sets an upper limit for the bias field of any model with an uncompensated interface.

For $K_{\rm A} = 0$ ($J_{\rm A} \neq 0$) the coercivity is always zero and the bias field is given by

$$H^{'}_{\rm eb} = \alpha\frac{J_{\rm A}J_{\rm eb}}{\sqrt{J^2_{\rm eb}+J^2_{\rm A}}}. \tag{10}$$

This equation is valid for any value of $J_{\rm eb}$, showing a saturation at $H^{'}_{\rm eb} = \alpha J_{\rm A}$ for large values of it (see figure 8). Equation (10) becomes equivalent to the MSBK model bias field with zero anisotropy at the FM film if we replace $J_{\rm A}$ by the partial domain wall energy, namely set $J_{\rm A} \to 2\sqrt{K_{\rm A}J_{\rm A}}$. In the general case when $K_{\rm A} \neq 0$ the coercivity is non-zero and the problem has to be treated numerically.

To understand the general behavior of the bias field as a function of $J_{\rm eb}$ let us first analyze the structure of the energy landscape given by equation (6) in the absence of external magnetic fields. Suppose that the system was cooled in the presence of an external field $H_{\rm CF}$ pointing in the positive y direction. Then, the energy has an absolute minimum, corresponding to both magnetic variables $\vec{S}$ and $\vec{\sigma}$ pointing in the positive y direction. We denote this minimum by $(\uparrow,\uparrow)$. If the anisotropy is weak, $K_{\rm A} < J_{\rm A}/2$, this minimum is unique. When $K_{\rm A} > J_{\rm A}/2$ a second (local) minimum appears corresponding to both variables $\vec{S}$ and $\vec{\sigma}$ pointing in the negative y direction. We denote this minimum by $(\downarrow,\downarrow)$. If $K_{\rm A} \gg J_{\rm A}$ the energy difference between the two minima is $\Delta E \approx 2J_{\rm A}$.

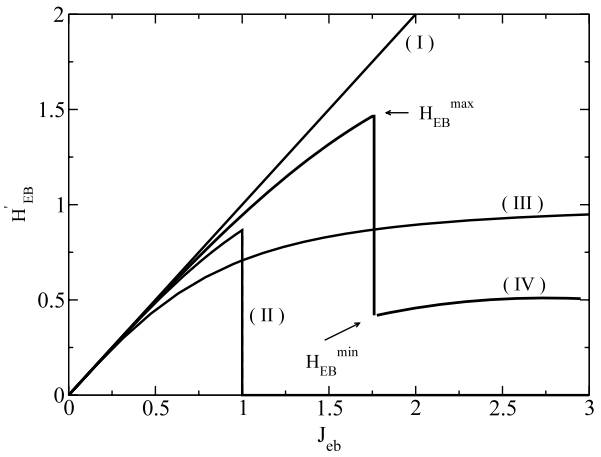

Figure 8. Bias field $H^{'}_{\rm EB}$ as a function of the interfacial exchange constant $J_{\rm eb}$ for different values of $J_{\rm A}$ and $K_{\rm A}$. (I) $J_{\rm A} = 0$ and $K_{\rm A} \gg 1$ (equation (9)); (II) $J_{\rm A} = 0$ and $K_{\rm A} = 1$ (equation (9)); (III) $J_{\rm A} = 1$ and $K_{\rm A} = 0$ (equation (10)); (IV) $J_{\rm A} = 1$ and $K_{\rm A} = 1$.

Let us consider now the descending branch of a hysteresis cycle, that is, we saturate the sample with an external field pointing in the positive y direction and decrease the field in regular steps until the sample is saturated in the opposite direction. The effect of the inverse applied field on the magnetic configuration depends on the relative strength of $j_{\rm eb} = J_{\rm eb}/J_{\rm A}$. If $j_{\rm eb} \ll 1$, the FM layer aligns with the field when $h \equiv H^{'}/J_{\rm A} \sim j_{\rm eb}$ but the AFM layer still points up, that is, the lower minimum $(\uparrow,\uparrow)$ changes its configuration to $(\uparrow,\downarrow)$. Therefore, $h_{\rm eb} \sim j_{\rm eb}$. When $j_{\rm eb} \sim 1$ (and therefore $h_{\rm eb} \sim 1$), the second minimum corresponding to the $(\downarrow,\downarrow)$ configuration becomes absolute. As $j_{\rm eb}$ increases further, the configuration $(\uparrow,\downarrow)$ remains as a local minimum, until above certain value of $j_{\rm eb}$ it loses stability. Hereafter we will consider $\alpha = 1$ (sc lattice) for simplicity.

The typical behavior of the bias field for finite values of $K_{\rm A}$ and $J_{\rm A}$ is illustrated in figure 8. For low values of $J_{\rm eb}$ the bias field shows a monotonic behavior, taking values between those given by equations (9) and (10). In this regime, the local minimum $(\uparrow,\downarrow)$ of the energy remains stable and the AFM layer forms a reversible quasi-domain wall, without inversion of its magnetization. Above some maximum value $J^{\rm max}_{\rm eb}$, the local minimum loses stability, giving rise to an irreversible inversion of the AFM layer magnetization and the system exhibits finite coercivity and a sudden drop in the bias field. However, at odds with the $J_{\rm A} = 0$ case, the bias field drops to a finite value, after which it increases again monotonically with $J_{\rm eb}$ (in agreement with the simulation results of section 3), due to the competition between the anisotropy and interaction of the AFM layer with the AFM bulk magnetization. For large enough values of $J_{\rm eb}$ the bias field saturates to a smaller value than for the $K_{\rm A} = 0$ case ($H^{'}_{\rm eb} \approx J_{\rm A}$). As $K_{\rm A}$ increases both the drop in the bias field and the value of $J_{\rm eb}$ where it happens increase.

Next we compared the predictions of the model with the Monte Carlo results. In figure 9 we illustrate the typical behavior for large values of the anisotropy. We see that, as temperature fluctuations decrease, the maximum in the bias

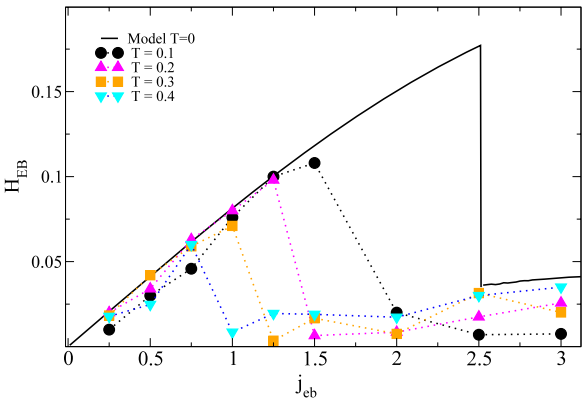

Figure 9. Bias field $H_{\rm EB}$ versus $j_{\rm eb}$ for different values of the temperature in the sc lattice, with the anisotropy value $K_{\rm A}/J_{\rm A} = 1.77$.

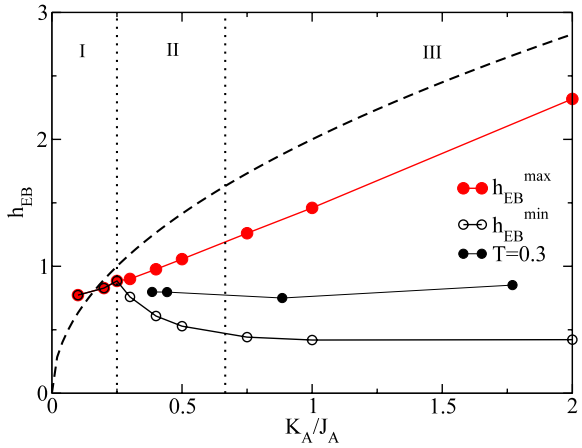

Figure 10. Reduced bias fields $h_{\rm EB}^{\rm max}$ and $h_{\rm EB}^{\rm min}$ as a function of the reduced anisotropy $K_{\rm A}/J_{\rm A}$. The dashed line is given by the MSBK model ($h_{\rm EB} = 2\sqrt{K_{\rm A}/J_{\rm A}}$).

field and the value of $j_{\rm eb}$ where it occurs increase, due to thermal activation. Of course, this depends on the time scales involved in the hysteresis loop, i.e. on the rate of variation of the field. If the rate of variation of the field is kept constant, the Monte Carlo results systematically approach the behavior predicted by the model as the temperature decreases, because the characteristic activation time systematically increases.

The range of anisotropy values for which the present approximation applies can be estimated as $K_{\rm A}/J_{\rm A} > \frac{2}{3}$ since it is known that in this range the domain wall width is equal to one lattice parameter [32]. When the anisotropy decreases, the domain wall thickness increases and more layers have to be considered for a proper description. For small enough values of the anisotropy a smooth domain wall is expected, so the behavior of the system should be well described by the MSBK model. The crossover to the regime of the MSBK model behavior can be estimated as the point where the energy of the domain wall equals the exchange energy at the antiferromagnet, namely $2\sqrt{K_{\rm A}\,J_{\rm A}} = J_{\rm A}$, which corresponds to $K_{\rm A}/J_{\rm A} = 0.25$. This is illustrated in figure 10, where we compare the maximum bias field $h_{\rm EB}^{\rm max} = H_{\rm EB}^{\rm max}/J_{\rm A}$ and the minimum after the drop $h_{\rm EB}^{\rm min} = H_{\rm EB}^{\rm min}/J_{\rm A}$ (see figure 8) with the bias field predicted by the MSBK model $h_{\rm EB} = 2\sqrt{K_{\rm A}/J_{\rm A}}$. The vertical dotted lines divide the graph into three regions of qualitatively different behavior. The region of validity of the present model ($K_{\rm A}/J_{\rm A} > \frac{2}{3}$) is marked as III. In this region a quasi-domain wall forms and, unlike for the continuous approximation where the internal domain wall spins change their orientation in a reversible way, now these spins can have an irreversible or hysteretical behavior, like when defects are present in the antiferromagnet [24].

In region I the continuous approach assumed in the MSBK model is valid. In region II neither the present model nor the MSBK model is expected to be valid, since the micromagnetic approach fails because the magnetization profile is not smooth on the atomic scale, but more than one interfacial plane is involved in the magnetization process at the interface. Moreover, we have seen from the Monte Carlo simulations that in this region, lattice structure effects can be very important. At the crossover point, $K_{\rm A}/J_{\rm A} = 0.25$, we see that $h_{\rm EB}^{\rm max} = h_{\rm EB}^{\rm min}$, i.e., the hysteresis disappears as expected.

It is worth noting that size effects in the antiferromagnet become relevant only in regions I and II, in particular when the thickness of the antiferromagnet is comparable to the domain wall size.

Let us analyze thermal effects in the bias field when the AFM domain wall is pinned, i.e., it is not able to propagate in the bulk of the AFM material. Suppose that the rate of variation of the field is small enough that the system can be assumed at thermodynamical equilibrium at every step of the loop. Then, the equilibrium behavior can be obtained by computing the partition function

$$\mathcal{Z}_n = \int_0^{2\pi} {\rm d}\phi_1 \cdots \int_0^{2\pi} {\rm d}\phi_n \exp\left(\beta\left(K_{\rm A}\sum_{i=1}^{n}\cos^2\phi_i - (-1)^n\sigma_0(T)\,\cos\phi_1 - \sum_{i=1}^{n-1}\cos(\phi_i-\phi_{i+1})\right)\right) \times \int_0^{2\pi} {\rm d}\theta\, {\rm e}^{\beta\vec{S}\cdot\vec{\omega}}, \tag{11}$$

where we have taken $\alpha J_{\rm A} = 1$, $\beta = 1/k_{\rm B}T$, ϕ_i and θ are the angles with respect to the y axis of the ith AFM and the FM spins, respectively, and $\vec{\omega} \equiv \vec{H}' + J\vec{\sigma}_n$ ($J \equiv \alpha J_{\rm eb}$). We assumed that the bulk AFM magnetization per layer is given by the mean field approximation [10, 33], namely

$$\sigma_0(T) = \mathcal{L}(z\beta\sigma_0(T)), \tag{12}$$

where $\mathcal{L}(x)$ is the Langevin function and z is the number of nearest neighbors which depends of the lattice structure $z = 6$ (8) for the sc, (bcc).

The last integral in equation (11) can be easily solved, obtaining the general expression (aside from an irrelevant multiplicative factor)

$$\mathcal{Z}_n = \int_0^{2\pi} {\rm d}\phi_1 \cdots \int_0^{2\pi} {\rm d}\phi_n \exp\left(\beta\left(K_{\rm A}\sum_{i=1}^{n}\cos^2\phi_i - (-1)^n \times \sigma_0(T)\cos\,\phi_1 - \sum_{i=1}^{n-1}\cos(\phi_i-\phi_{i+1})\right)\right) \times I_0(\beta\,\omega(\phi_n)), \tag{13}$$

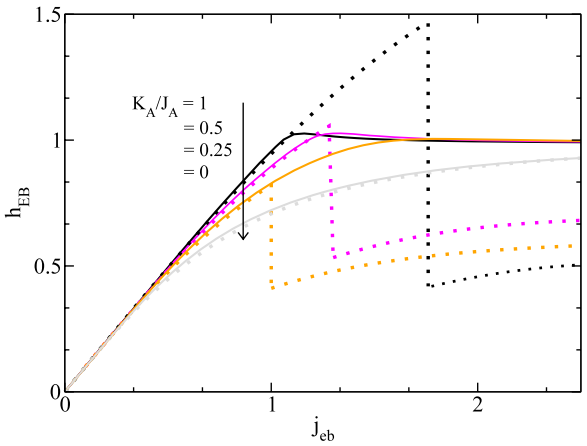

Figure 11. Reduced bias field $h_{\rm EB}$ versus $j_{\rm eb}$ for different values of $K_{\rm A}/J_{\rm A}$. Full lines: equilibrium curves for $n = 1$ at $T/J_{\rm A} = 0.1$. Dotted lines: $T/J_{\rm A} = 0$.

where $I_\nu(x)$ is the modified Bessel function and $\omega(\phi) = \sqrt{H'^2 + J^2 + 2\,J\,H'\cos\,\phi}$. The average magnetization in the FM layer can be obtained as $m^{\rm F} \equiv \langle\cos\,\theta\rangle = \frac{1}{\beta\,\mathcal{Z}_n}\frac{\partial \mathcal{Z}_n}{\partial H'}$ and the magnetization at the jth AFM layer, $m_j^{\rm AF} \equiv \langle\cos\,\phi_j\rangle$, can be computed in a similar way. Solving numerically the previous equations as functions of the applied field and temperature we obtained the dependence of the bias field on temperature. We considered the cases $n = 1$ and 2. No qualitative differences were observed. We present here the results for $n = 1$, which are adequate for illustrating the general behavior.

In figure 11 we compare the equilibrium reduced bias field $h_{\rm EB}$ as a function of $j_{\rm eb}$ at low temperatures (full lines) with the zero-temperature curves obtained from equation (5) (dotted lines) for several anisotropy values. One can see that for low interfacial interaction strength $j_{\rm eb} \ll 1$ the temperature has little effect on the bias field. In both cases an increase in the anisotropy enlarges the range of the linear behavior expected in the strong anisotropy limit (see figure 8). This can be easily understood if we recall that in this regime the system behaves reversibly even at zero temperature. In other words, in both cases the behavior of the system is governed by the absolute minimum of the energy, so the relation $j_{\rm eb} \sim h_{\rm eb}$ still holds, no matter what the value of the anisotropy is.

The main difference appears for high values of $j_{\rm eb}$. First of all, the drop in $h_{\rm EB}$ observed in the $T = 0$ curves is absent in the thermalized curves, since of course at equilibrium there is no coercivity. Second, the bias field $h_{\rm EB}$ saturates to the value $h_{\rm EB} \sim 1$ as $j_{\rm eb}$ increases ($j_{\rm eb} > 1$) independently of the anisotropy, contrasting with the case for the $T = 0$ curves where the maximum value of $h_{\rm EB}$ increases with the anisotropy. When $j_{\rm eb} \gg 1$ the applied field changes the relative depth of the two energy minima. When $h \sim 1$ the two minima have the same energy and the magnetization at the FM layer inverts: $m^{\rm F} = 0$, independently of the anisotropy. Therefore, $h_{\rm eb} \sim 1$, i.e. the bias field reaches the saturation value observed in figure 11. On the other hand, the bias field at zero temperature continuously grows with the anisotropy due to the fact that the energy barriers between the minima increase with the anisotropy.

It is worth remarking that, even at equilibrium, the bias field exhibits a maximum at $j_{\rm eb} \sim 1$ for large values of the anisotropy.

5. Discussion

We found that, in fully uncompensated interfaces, the bias field displays a non-monotonic dependence on the interfacial interaction strength. Depending on the temperature and on the anisotropy to exchange ratio $K_{\rm A}/J_{\rm A}$ of the antiferromagnet, $H_{\rm EB}$ can present a peak as a function of $J_{\rm eb}$. In particular, the peak is observed at low temperatures and high enough ratios $K_{\rm A}/J_{\rm A}$. When it is present, the peak position moves toward lower values of $J_{\rm eb}$ as the temperature is increased, while below a certain temperature (low compared with the blocking temperature) the peak disappears. The peak is associated with the onset of coercivity, i.e. with the appearance of hysteresis for large values of $J_{\rm eb}$.

When $K_{\rm A}/J_{\rm A} > \frac{2}{3}$ (region III in figure 10), the behavior of the bias field is completely determined by the dynamics of the interfacial AFM layer. For low values of $J_{\rm eb}$ the interfacial layer rotates coherently forming a quasi-domain wall that changes reversibly with the applied field. In this regime the bias field increases almost linearly with $J_{\rm eb}$ and thermal effects are negligible. Above a certain critical value of $J_{\rm eb}$ the quasi-domain wall loses stability and the magnetization of the interfacial AFM layer changes irreversibly. In other words, the bias field is controlled by the stability of the interfacial layer. This scenario, supported by both the Monte Carlo simulations and the simple layered model introduced here, explains why the bias field can be drastically reduced by increasing the interfacial interaction strength (figure 2). Also in this regime ($K_{\rm A}/J_{\rm A} > \frac{2}{3}$), the behavior of the bias field is independent of the lattice structure. In other words, a change in the crystalline structure is just equivalent to a rescaling of the effective anisotropy of the antiferromagnet.

When $K_{\rm A}/J_{\rm A} < \frac{2}{3}$, the system can still exhibit hysteresis and a peak in the bias field (region II in figure 10), but the width of the domain wall increases as $K_{\rm A}/J_{\rm A}$ decreases. In this case the bias field is controlled by the intrinsic pinning due to the anisotropy. Namely, for large values of $J_{\rm eb}$ the bias field reduces because of the depinning of this domain wall, which depends strongly on the lattice structure. In particular, preliminary results showed that the pinning is stronger in the bcc than in the sc lattice, due to canting effects in the AFM layers. A detailed study of such an effect is underway and will be published elsewhere.

In both regimes (II and III) the maximum bias field is smaller than the value predicted by the MSBK model. These results offer certain insights into experimental findings for FeF_2 systems [8, 9] ($K_{\rm A}/J_{\rm A} > \frac{2}{3}$), where in a fully uncompensated interface the bias field is much lower than expected. In particular, it becomes noticeable at very low temperatures. According to our results, if the interfacial strength interaction is strong the bias field becomes non-null only at very low temperatures compared with the Néel temperature of the antiferromagnet.

Summarizing, depending on the anisotropy to exchange ratio K_A/J_A the bias field is controlled either by the intrinsic pinning of an extended domain wall parallel to the interface (low anisotropy regime) or by the stability of the first AFM interfacial plane near the interface (sharp domain wall limit).

Acknowledgments

This work was partially supported by grants from CONICET (Argentina), Agencia Córdoba Ciencia (Argentina), SeCyT, and Universidad Nacional de Córdoba (Argentina).

References

[1] Nogués J, Sort J, Langlais V, Skumryev V, Suriñach S, Muñoz J S and Baró M D 2005 Exchange bias in nanostructures *Phys. Rep.* **422** 65–117
[2] Nogués J and Schuller I K 1999 Exchange bias *J. Magn. Magn. Mater.* **192** 203–32
[3] Meiklejohn W H and Bean C P 1956 New magnetic anisotropy *Phys. Rev.* **102** 1413–4
[4] Kiwi M 2001 Exchange bias theory *J. Magn. Magn. Mater.* **234** 584–95
[5] Berkowitz A E and Kentaro T 1999 Exchange anisotropy—a review *J. Magn. Magn. Mater.* **200** 552–70
[6] Radu F and Zabel H 2008 *Magnetic Heterostructures; Advances and Perspectives in Spin Structures and Spin Transport* (*Springer Tracts in Modern Physics* vol 227) (Berlin: Springer)
[7] Takano K, Kodama R H, Berkowitz A E, Cao W and Thomas G 1997 Interfacial uncompensated antiferromagnetic spins: role in unidirectional anisotropy in polycrystalline $Ni_{81}Fe_{19}$/CoO bilayers *Phys. Rev. Lett.* **79** 1130
[8] Moran T J, Nogués D, Lederman J and Schuller I K 1998 Perpendicular coupling at Fe–Fe_2 interfaces *Appl. Phys. Lett.* **5** 617
[9] Nogués J, Moran T J, Lederman D, Schuller I K and Rao K V 1999 Role of interfacial structure on exchange-biased FeF_2–Fe *Phys. Rev.* B **59** 6984–93
[10] Scholten G, Usadel K and Nowak U 2005 Coercivity and exchange bias of ferromagnetic/antiferromagnetic multilayers *Phys. Rev.* B **71** 064413
[11] Leighton C, Suhl H, Pechan M J, Compton R, Nogués J and Schuller I K 2002 Coercivity enhancement above the Néel temperature of an antiferromagnet/ferromagnet bilayer *J. Appl. Phys.* **92** 1483
[12] Ohldag H, Shi H, Arenholz E, Stöhr J and Lederman D 2006 Parallel versus antiparallel interfacial coupling in exchange biased Co/FeF_2 *Phys. Rev. Lett.* **96** 1–4
[13] Suess D, Schrefl T, Scholz W, Kim J -V, Stamps R L and Fidler J 2002 Micromagnetic simulation of ferromagnetic/antiferromagnetic structures *IEEE Trans. Magn.* **38** 2397
[14] Suess D, Kirschner M, Schrefl T, Fidler J, Stamps R L and Kim J-V 2003 Exchange bias of polycrystalline antiferromagnets with perfectly compensated interfaces *Phys. Rev.* B **67** 054419
[15] Dorfbauer F, Suess D, McCord J, Kirschner M, Schrefl T and Fidler J 2005 Micromagnetic simulations of asymmetric magnetization reversal in exchange biased bilayers *J. Magn. Magn. Mater.* **291/292** 754–7
[16] Billoni O, Tamarit A and Cannas S 2006 Monte Carlo simulations of a ferromagnetic–F_2Fe system *Physica* B **384** 184–6
[17] Spray J and Nowak U 2006 Exchange bias in ferromagnetic/antiferromagnetic bilayers with imperfect interfaces *J. Phys. Appl. Phys.* D **39** 4536–9
[18] Lederman D, Ramírez R and Kiwi M 2004 Monte Carlo simulations of exchange bias of ferromagnetic thin films on FeF_2(110) *Phys. Rev.* B **70** 184422
[19] Misra A, Nowak U and Usadel K D 2004 Structure of domains in an exchange-bias model *J. Appl. Phys.* **95** 1357
[20] Mitsumata C, Sakuma A and Fukamichi K 2003 Mechanism of exchange-bias field in ferromagnetic and antiferromagnetic bilayers *Phys. Rev.* B **68** 014437
[21] Sakurai Y and Fujiwara H 2003 Numerical simulation of unidirectional anisotropy in ferro(F)/antiferromagnetic(AF) exchange coupled layers with a compensated AF-interface *J. Appl. Phys.* **93** 8615
[22] Nowak U, Usadel K D, Keller J, Miltényi P, Beschoten B and Güntherodt G 2002 Domain state model for exchange bias. I. Theory *Phys. Rev.* B **66** 014430
[23] Nowak U, Misra A and Usadel K D 2002 Modeling exchange bias microscopically *J. Magn. Magn. Mater.* **240** 243–7
[24] Kim J-V and Stamps R L 2005 Hysteresis from antiferromagnet domain-wall processes in exchange-biased systems: magnetic defects and thermal effects *Phys. Rev.* B **71** 094405
[25] Meiklejohn W H 1962 Exchange anisotropy—a review *J. Appl. Phys.* **33** 1328–35
[26] Mauri D, Siegmann H C, Bagus P S and Kay E 1988 Simple model for thin films exchange coupled to an antiferromagnetic substrate *J. Appl. Phys.* **62** 3047–9
[27] Wang L, Ding J, Kong H, Li Y and Feng Y 2001 Monte Carlo simulation of a cluster system with strong interaction and random anisotropy *Phys. Rev.* B **64** 214410
[28] Billoni O, Cannas S and Tamarit F 2005 Spin-glass behavior in the random-anisotropy Heisenberg model *Phys. Rev.* B **72** 8–11
[29] Nowak U, Chantrell R and Kennedy E 2000 Monte Carlo simulation with time step quantification in terms of Langevin dynamics *Phys. Rev. Lett.* **84** 163–6
[30] Tsai S H, Landau D P and Schulthess T C 2002 Monte Carlo simulations of ordering in ferromagnetic–antiferromagnetic bilayers *J. Appl. Phys.* **91** 6684–6
[31] Geshev J 2000 Analytical solutions for exchange bias and coercivity in ferromagnetic/antiferromagnetic bilayers *Phys. Rev.* B **62** 5627–33
[32] Barbara B 1973 Propriétés des parois ètroites dans les substances ferromagnétiques a forte anisotropie *J. Physique* **34** 1039
[33] Nascimento F, Dantas A, Oliveira L, Mello V, Camley R and Carriço A 2009 Thermal hysteresis of ferromagnetic/antiferromagnetic compensated bilayers *Phys. Rev.* B **80** 144407